Paper: ASAT-15-106-CV

15th International Conference on
AEROSPACE SCIENCES & AVIATION TECHNOLOGY,
ASAT - 15 – May 28 - 30, 2013, Email: asat@mtc.edu.eg ,
Military Technical College, Kobry Elkobbah, Cairo, Egypt,
Tel: +(202) 24025292 –24036138, Fax: +(202) 22621908

Load Width Effect on The Shear Behavior of Prestressed Hollow Core Slabs

A. N. Deeb*, M. A. Z. Tarkhan†, E. M. El-Tehewy‡

Abstract: Instead of performing a costly experimental study to find out whether the effect of different factors on the prediction of shear behavior of hollow core slabs, a numerical model can be developed. From the numerical analysis, the effective of load width across the slab width can be derived.
This paper present the shear behavior of prestressed hollow core slabs and examined the effect of load width (in absence of concrete topping and filling of cores) on their effective shear behavior. In the present investigation, physical tests and 3-D finite element models were developed using the general-purpose finite element software ANSYS 11.0 to simulate the behavior of tested slabs. The specimens used in this research have a depth of 150 *mm* and the numerical models are calibrated using the data obtained from physical experiments. The ANSYS finite element analysis results are compared with the experimental data of two prestressed hollow core slabs. The comparisons are made for load-deflection curves, failure loads and crack patterns, respectively. The accuracy of the finite element models is assessed by comparison with the experimental results, which are in good agreement.

Keywords: Prestressed hollow core slabs; Shear failure; Finite-element analysis; Pre-stressing strands; Reinforced concrete; ANSYS 11.

1. Introduction

Precast, prestressed hollow core slabs (PHC slabs) are among the most commonly used load bearing concrete elements in the world. They are widely used in floors and roofs of office, residential, commercial and industrial buildings [1]. These units were developed in the 1950s, when long-line prestressing techniques evolved. For more than 30 years, the type of units produced changed little. Extensive research performed in Europe in the 1980s, led to technology advances allowing the economical production of hollow core units [2].
In order to verify the as-cast shear capacity of PHC slabs, a suitable test set-up must be designed to take into account all variables, which may contribute either negatively or positively to the shear capacity of the slabs [3].
The selection of the type of the applied load used for a shear test (uniform or concentrated) can also have an effect on the member behavior. A common approach for shear testing is to use a concentrated load, resulting in shear forces that are essentially constant between the load and the support reaction [3].
Two full-scale tests on one-way floor systems of 3.5 *m* lengths, 1.2 *m* widths and 0.15 *m* height are performed in order to investigate the shear capacity behavior of PHC slabs and to check the obtained results of ANSYS program.

* Syrian Armed Forces, Syria, haidra_deeb@yahoo.com
† Assoc. Prof., Helwan University, Cairo, Egypt.
‡ Egyptian Armed Forces, Egypt.

The finite element (FE) method is now well accepted as the most powerful general technique for the numerical solution of a variety of engineering problems. In the realm of linear analysis, the FE method is now widely used as a design tool. In addition, the finite element modeling (FEM) is a very useful and economic tool to study the complex behavior of structural elements such as shear resistance of PHC slabs. It was observed during the literature review that FE method helped researchers [4, 5, 6] to derive very important conclusions about the effect of the studied parameters, which were not covered in the experimental study.
Before application of nonlinear methods, in design stage it is commonly that, the accuracy and reliability of the proposed models, have to be established beyond doubt. The development of improved element characteristics and more efficient nonlinear solution algorithms as well as the experience gained in their applications to engineering problems has ensured that nonlinear FE analysis can now be performed with some confidence. Therefore, this paper was dedicated to the nonlinear analysis using three-dimensional FEM to simulate the laboratory tests and to derive conclusions about the effect of different parameters. The finite element software package, ANSYS (version 11) [7] was used for this purpose. Using the provided structural features in that package, a model for PHC slabs was constructed and used to conduct a parametric study. The finite elements model uses a smeared cracking approach to model the reinforced concrete and link spar 8 elements to model the strand composites. The prestressing force is applied as joint loads. This model provides a valuable supplement to the laboratory investigations.

2. Test Programme

Two prefabricated hollow core slabs are tested under concentrated load. The slabs have the same cross-section and prestressing strand, with dimensions of 3.5 m lengths, 1.2 m widths and 0.15 m heights, respectively. Each slab has twelve elliptical-shaped openings, and one oblong-shaped in the mid of slabs width. It is reinforced by eight pre-stressing seven-wire strands by along its bottom surface, as shown in Fig.1. Tables 1 and 2 summarize the details of the slab properties and prestressing strands respectively.

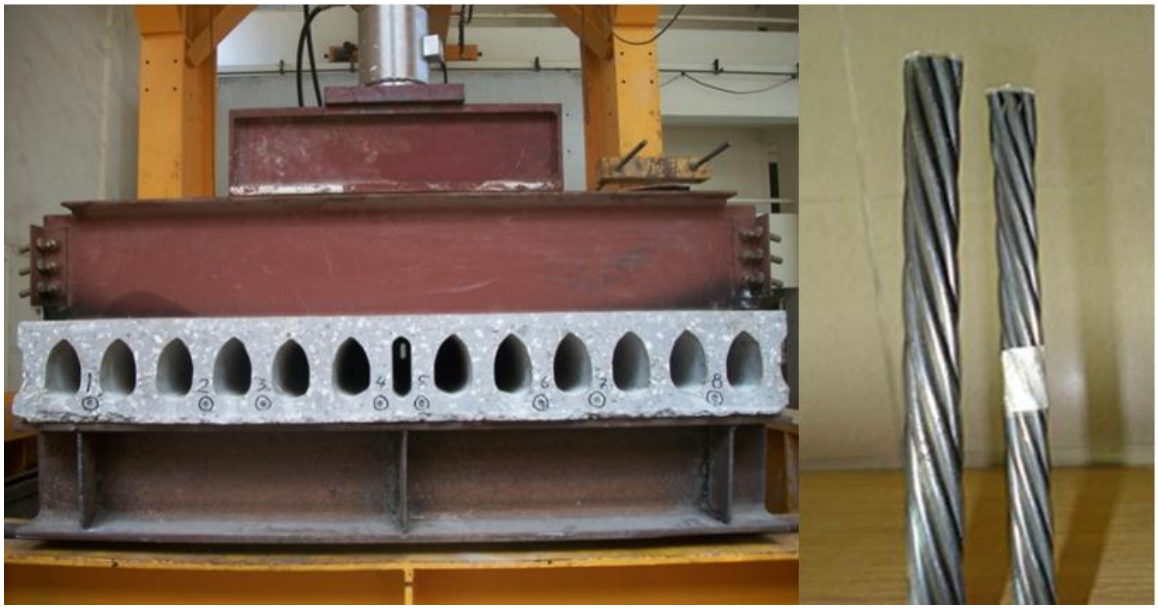

Fig.1: Details for tested PHC slabs and prestressing strands

Table 1: Properties of hollow-core slab

Slabs	Slab Length (mm)	Nominal Slab Depth (mm)	Slab Section Area (cm^2)	Compressive Strength (f_{cu}) (N/mm^2)	Shear span (a) (mm)	Prestressing Force (kN)
SA	3500	150	1234.4	43.57	300	518
SB	3500	150	1234.4	43.57	450	518

Table 2: Properties of pre-stressing seven-wire strands

Strands	Cross section (mm^2)	Nom. Diameter (mm)	Mass (g/m)	Breaking load (kN)	Ultimate strength (N/mm^2)	Yield strength (N/mm^2)	Modulus of elasticity (N/mm^2)
7-wire	54.84	9.53	432	102.3	1860	1679	197500

The PHC slabs are supported on the top flanges of two I-beams and loaded with a concentrated load P, as shown in Fig.2. Figure 3 shows the details of the tested hollow core slabs, the load acts on an I-beam with a length equal to the width of tested slab at the distance (a) of 2h (300 mm) for tested slab SA and 3h (450 mm) for tested slab SB, where (a) is the distance from the centre line of the applied load to the middle of the bearing surface, and (h) is the slab thickness, respectively. The load was applied in increments of 10 kN .

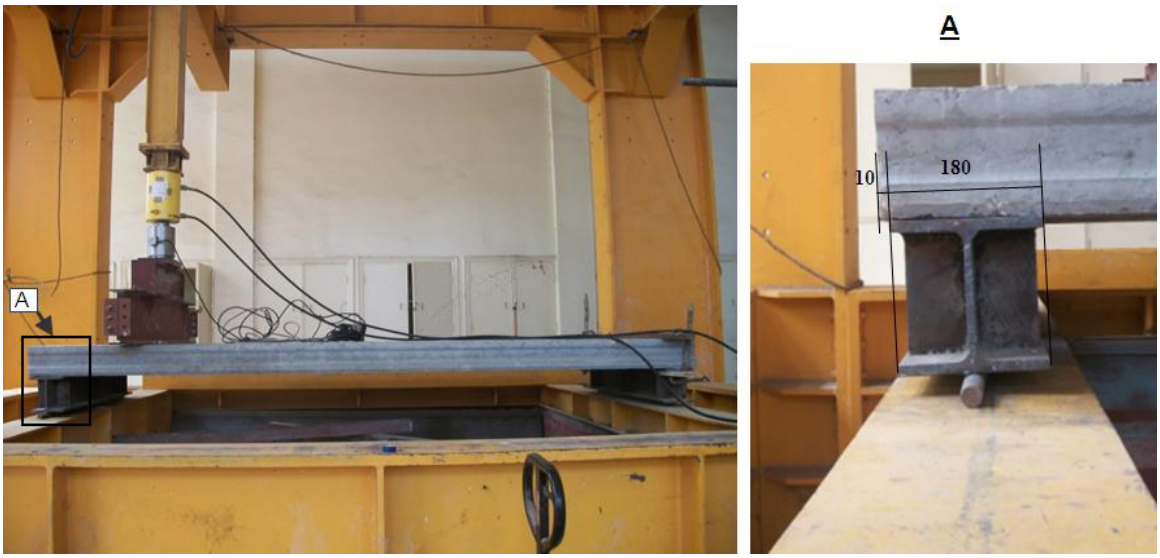

Fig.2: Test set-up and instrumentation for the tested PHC slabs

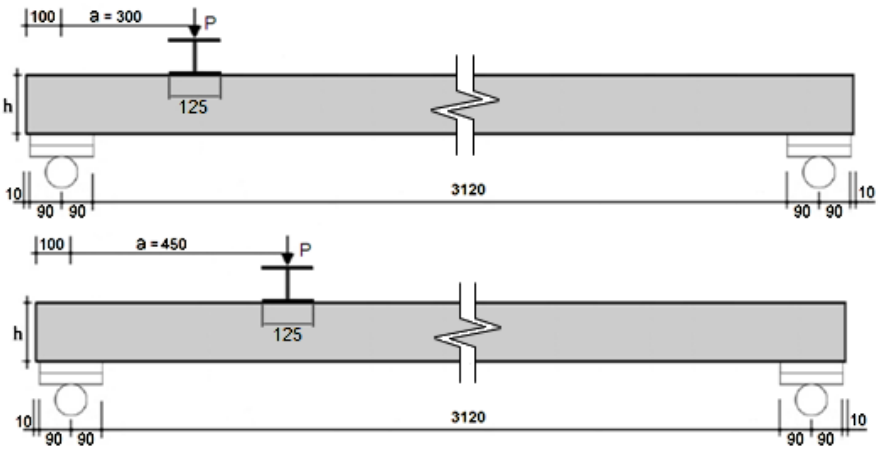

Fig.3: Loading of tested hollow-core slabs SA and SB

3. Finite Element Modeling

To simulate the behavior of the tested PHC slabs under the effect of a concentrated load, the finite element software ANSYS 11 is used. Two types of elements SOLID65 and LINK8 are selected to model concrete and prestressed steel tendons, respectively. The material properties defined for each type of element in the finite element model are based on the standard test.

3.1. Concrete

In this study, The SOLID65 element is used to simulate the behavior of concrete. This element is capable of modeling cracking in tension and crushing in compression. It also has the features of plastic deformation and creep. The most important aspect of this element is its capability of handling nonlinear material properties.

The SOLID65 element has eight nodes with three degrees of freedom at each node (translations in the nodal x, y, and z directions). The geometry, node locations, and the coordinate system for this element are shown in Fig.4, [7].

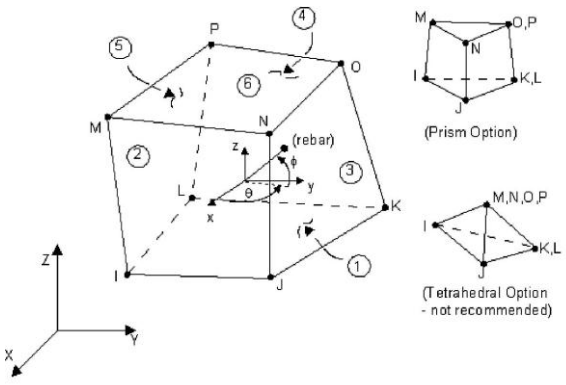

Fig. 4: The used (SOLID65) 3-D concrete element [7]

The additional concrete material data needed for SOLID65 element are shear transfer coefficients, tensile stresses and compressive stresses. Typical shear transfer coefficients range from zero for a smooth or open crack to one for rough or closed crack. For concrete, (ANSYS) requires input data for material properties as follows:

- The corresponding elastic modulus (E_C), (calculated as $E_C = 4400\sqrt{f_c^{'}} = 26764 MPa$)
- Ultimate uniaxial compressive strength ($f_c^{'}$); ($f_c^{'} = 0.85 \times 43.57 = 37 MPa$)
- Ultimate uniaxial tensile strength (f_{ctr}), (calculated as $f_{ctr} = 0.6\sqrt{f_c^{'}} = 3.65 MPa$)
- Poisson's ratio (ν) = 0.2
- Shear transfer coefficient (β_t); the shear transfer coefficient used in this study was taken equal to 0.2 for open cracks and 0.9 for closed cracks.
- Compressive uniaxial stress-strain relationship for concrete.

The concrete is assumed homogeneous and initially isotropic [7]. The compressive uniaxial stress-strain relationship for concrete model is obtained by using the following equations to compute the multi-linear isotropic stress-strain curve for the concrete as demonstrated [8] and shown in Fig.5.

$$f_c = \varepsilon E \quad \text{For} \quad 0 \le \varepsilon \le \varepsilon_1 \tag{1}$$

$$f_c = \frac{\varepsilon E}{1 + (\frac{\varepsilon}{\varepsilon_0})^2} \quad \text{For} \quad \varepsilon_1 \le \varepsilon \le \varepsilon_0 \tag{2}$$

$$f_c = f_c^{'} \quad \text{For} \quad \varepsilon_0 \le \varepsilon \le \varepsilon_u \tag{3}$$

$$\varepsilon_0 = \frac{2f_c^{'}}{E} \quad , \quad \varepsilon_1 \text{ at } 0.3f_c^{'} \tag{4}$$

where:

f_c Stress at any strain ε . (N/mm^2).

$f_c^{'}$ Characteristic compressive strength for concrete at 28 days. (N/mm^2).

ε_0 Strain at the ultimate compressive strength. ($f_c^{'}$).

The solution output associated with element SOLID65 are the nodal displacements included in the overall nodal solution and other additional element output such as concrete nonlinear integration point solution since cracking or crushing may occur at any integration point. In addition, the cracking or crushing status for each integration point can be reviewed in all directions, where the cracking plane is defined by two cracking angles ($\theta_{cr} \& \phi_{cr}$) as shown in Fig.6, [7].

3.2. Pre-Stressing Strands

In the present study, the LINK8 element is used to model the prestressed steel tendons. This 3-D spar element is a uniaxial tension-compression element that is capable of modeling plastic deformations. Element LINK8 is defined by two nodes, the cross-sectional area, an initial strain, and the material properties. The pre-stressing strands of area $54.84 mm^2$ are used. The yield strength, ultimate strength, and modulus of elasticity were 1679, 1860, and $197500 N/mm^2$, respectively. A Poisson's ratio of 0.3 is used for the prestressing strand. The geometry, node locations, and the coordinate system for this element are shown in Fig.7, [7]. In addition, Figure 8 shows the stress-strain curve of prestressing strands.

The prestressing force is applied as nodal forces distributed uniformly along the development length L_d of the prestressing strands as demonstrated [9]. In the presented study in variance with [9] and according to ACI 318-08 code [10], the development length turned out to be about $L_d = 1.3\ m$ as shown in Fig.9.

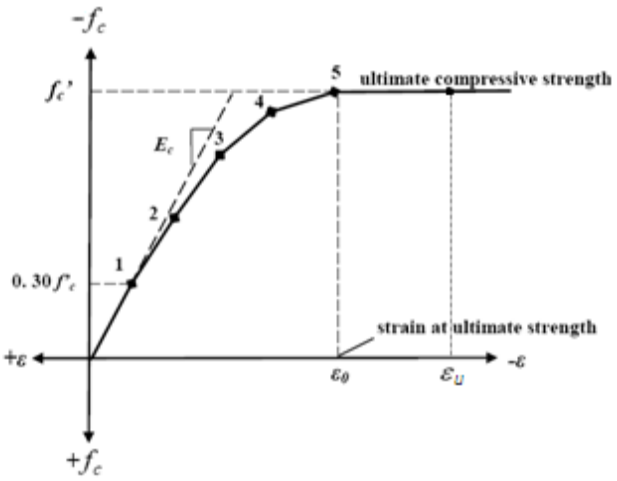

Fig.5: Simplified compressive uniaxial stress-strain curve of concrete [8]

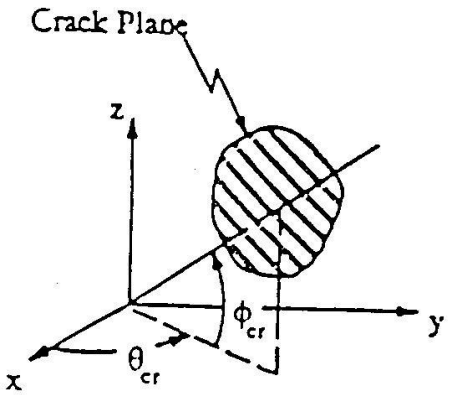

Fig.6: Cracking plane in (SOLID65) element [7]

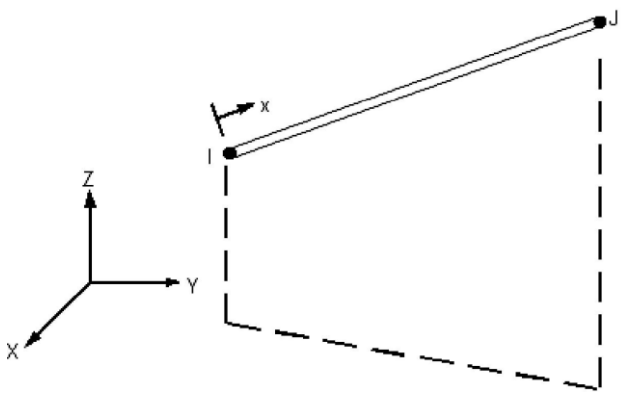

Fig.7: Geometry, node location, and coordinate system of 3-D spar element (LINK8) [7]

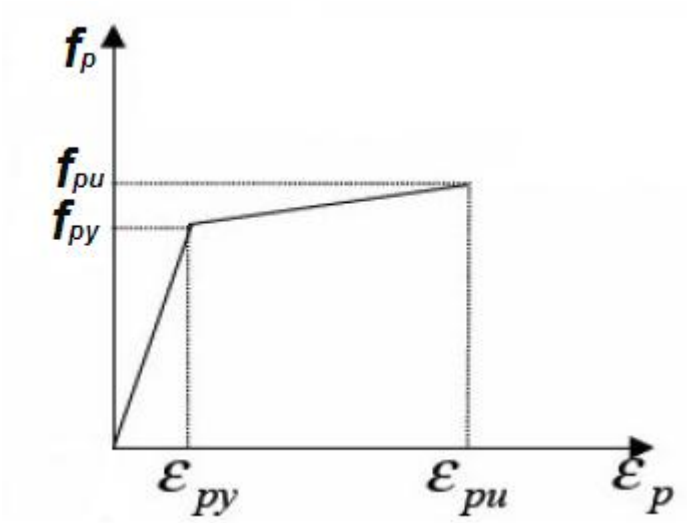

Fig.8: Stress-strain curve for pre-stressing strands

3.3. Finite Element Model

The developed numerical model for the PHC slabs and the typical dimensions of the finite element model are shown in Fig.9.

The mesh layout, which used in the present model, is the same in all analytical models. Using a single layer of integrated elements to represent the depth of the slab is obviously incorrect; therefore, six elements are used to represent the depth of the slab. The geometry of the mesh layout is shown in Fig.10.

The load was applied on the nodes of the upper surface of PHC slabs in increments of $10\,kN$ to simulate the experimental test. In the linear range, this load increment was divided into 2 sup-steps. Close to the failure load, increment was divided into 10 sup-steps.

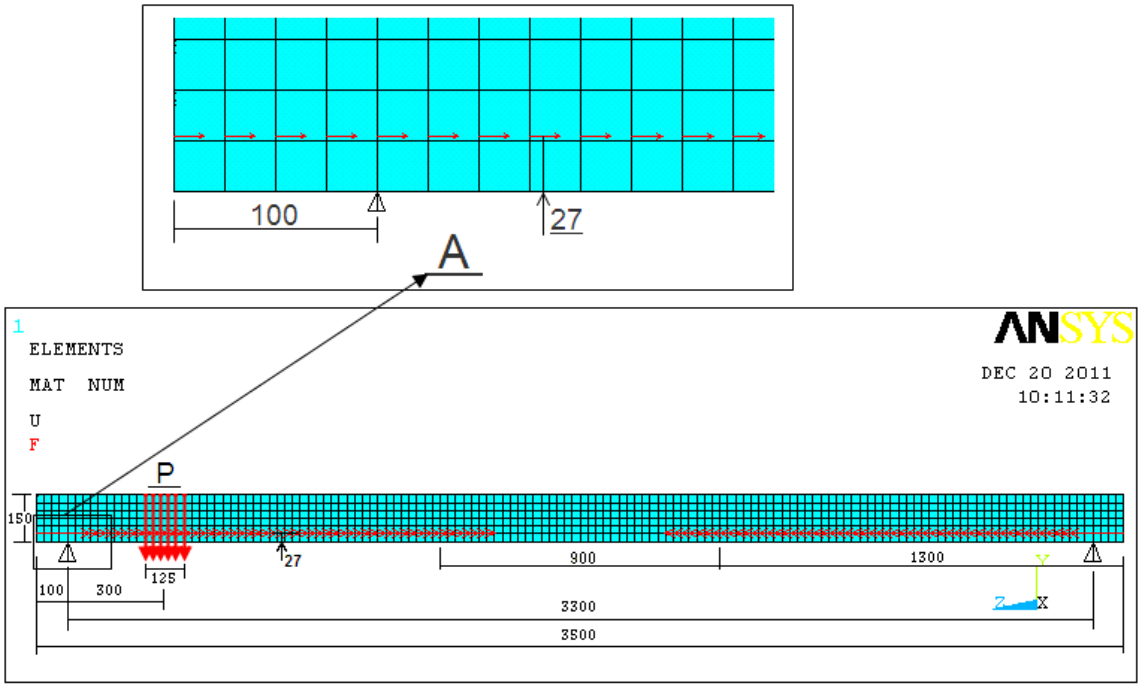

Fig.9: Finite element model for pre-stressed hollow core slab (Shows applied prestressing load)

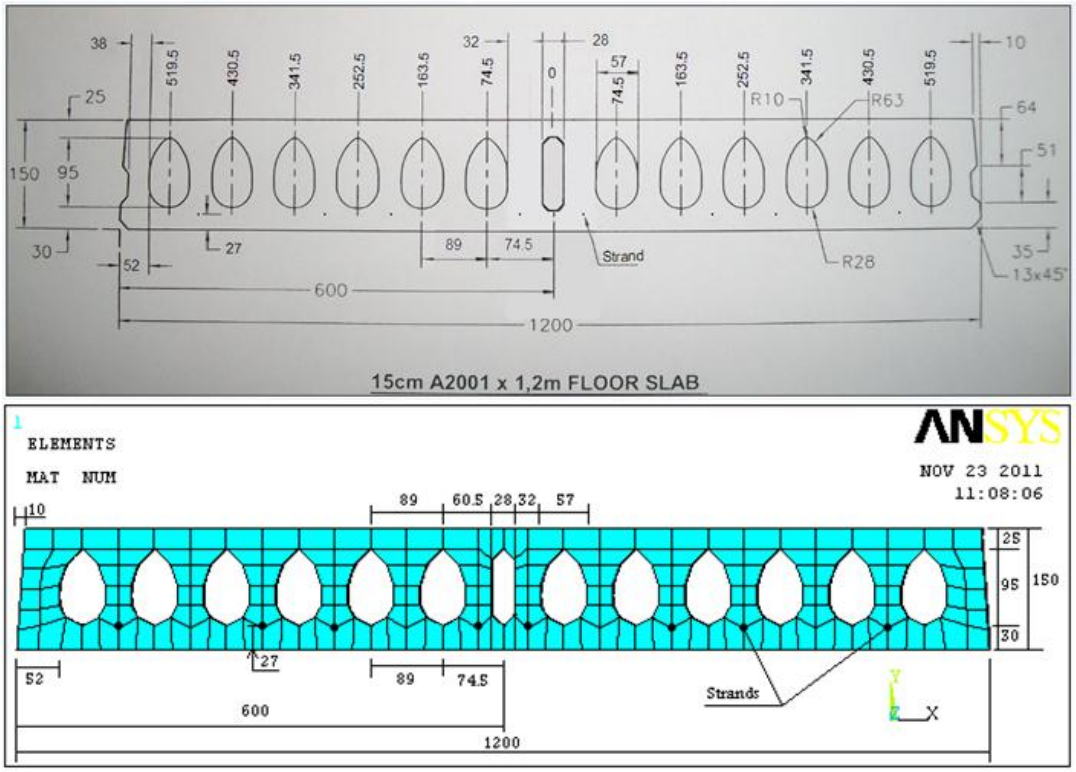

Fig.10: Typical dimensions of the tested PHC slabs and strands

4. Model Verification

4.1. Load Deflection Curves

The deflections of the tested PHC slabs at each applied load increment were taken from the output results to construct the load-deflection curves and the crack propagation was observed for each model. The failure point is determined in the analytical model at the load value, where the computer program indicates suddenly large deflection. The maximum nominal load of a specimen was used as an index in the comparison of the two sets of results.

For all models, the load-deflection curves of concrete were recorded at middle width of slabs on the bottom surface at two locations: first directly under vertical load, second at point A (were the maximum deflection occurred) as shown in Fig.11.

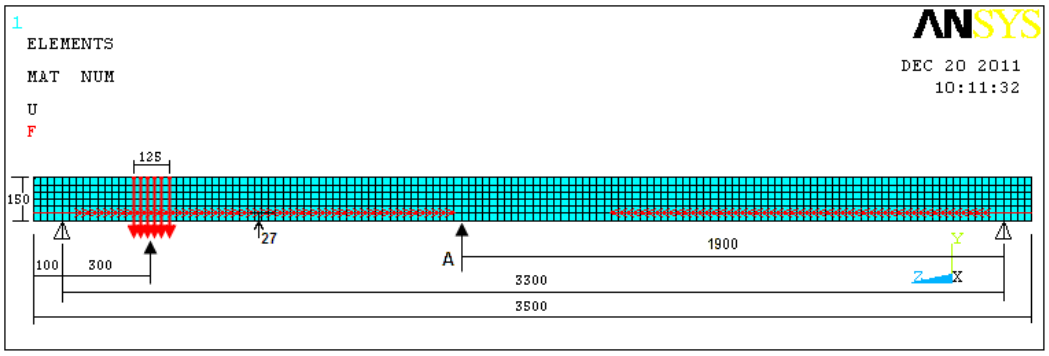

Fig.11: Location of the recorded deflection (Under vertical load and at point A)

A comparison between the experimental and numerical load-deflection curves for the tested PHC slabs are shown in Figures 12 ~ 15, respectively. It is clear that the failure mode of the analytical model is similar to that in the experimental model, and behaves in the same manner. The curves show good agreement between the finite element analysis and the experimental results throughout the entire range of behavior and failure mode.

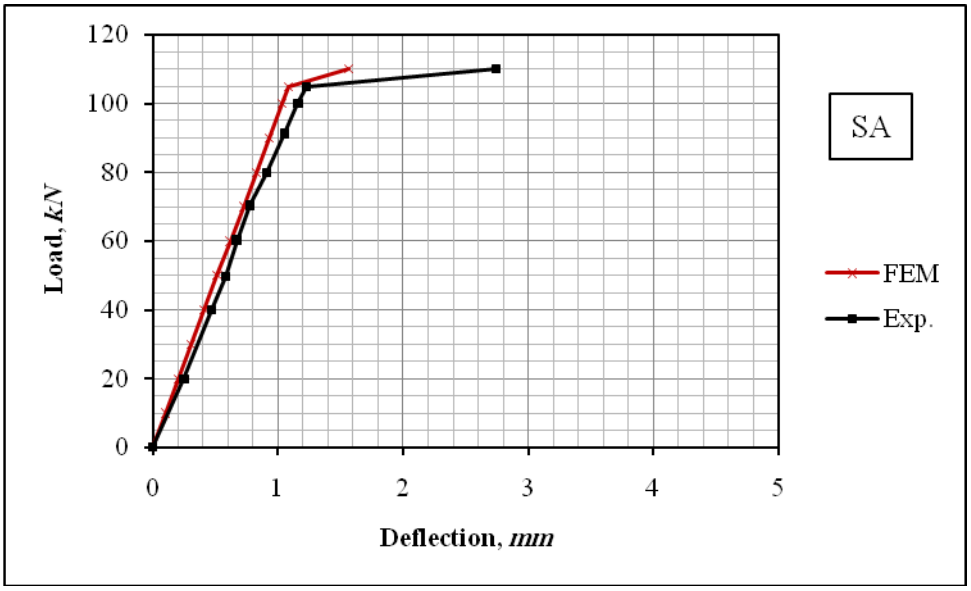

Fig.12: Load-deflection curves for tested PHC slab SA
(At point under vertical load)

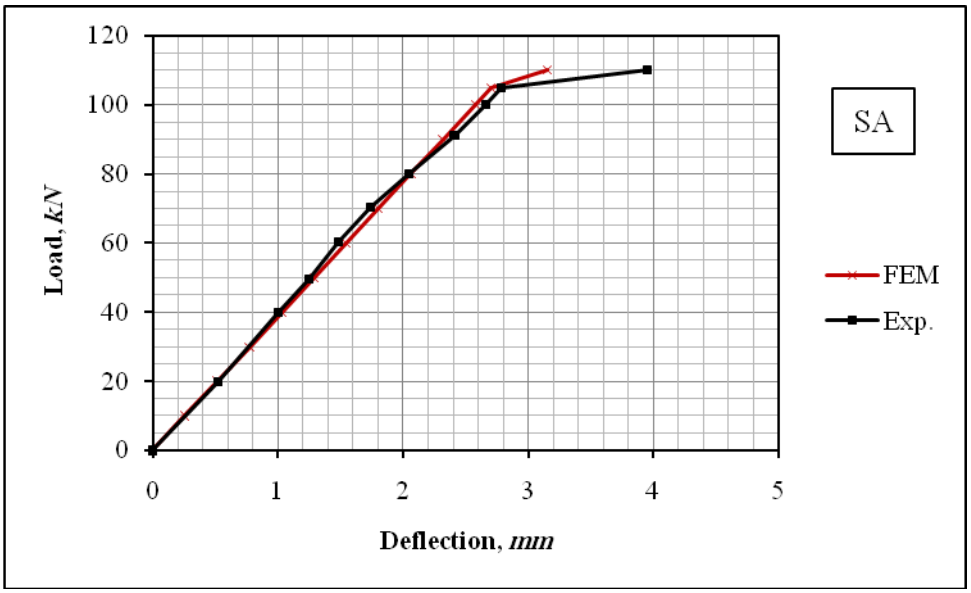

Fig.13: Load-deflection curves for tested PHC slab SA
(At point A of max. deflections)

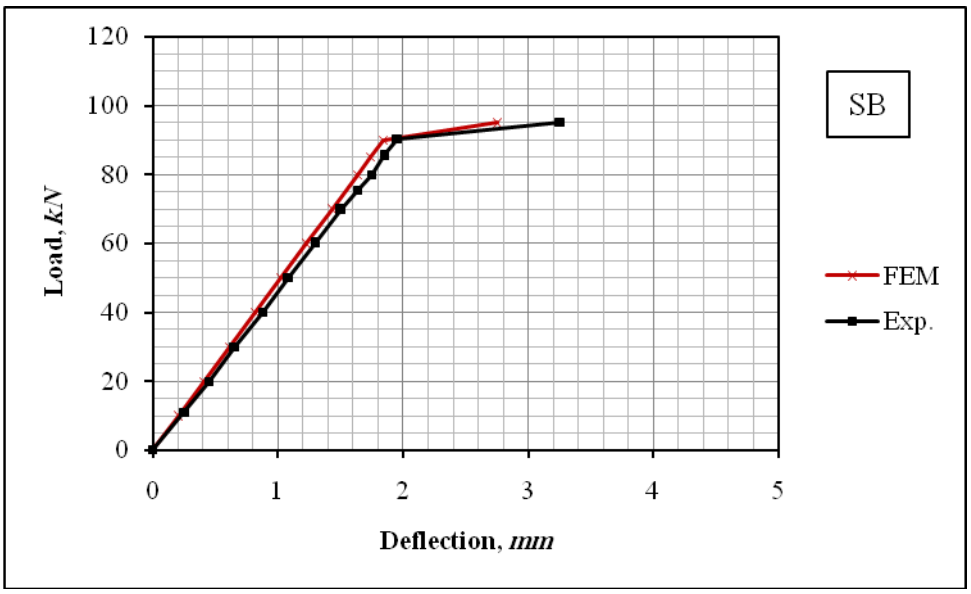

Fig.14: Load-deflection curves for tested PHC slab SB (At point under vertical load)

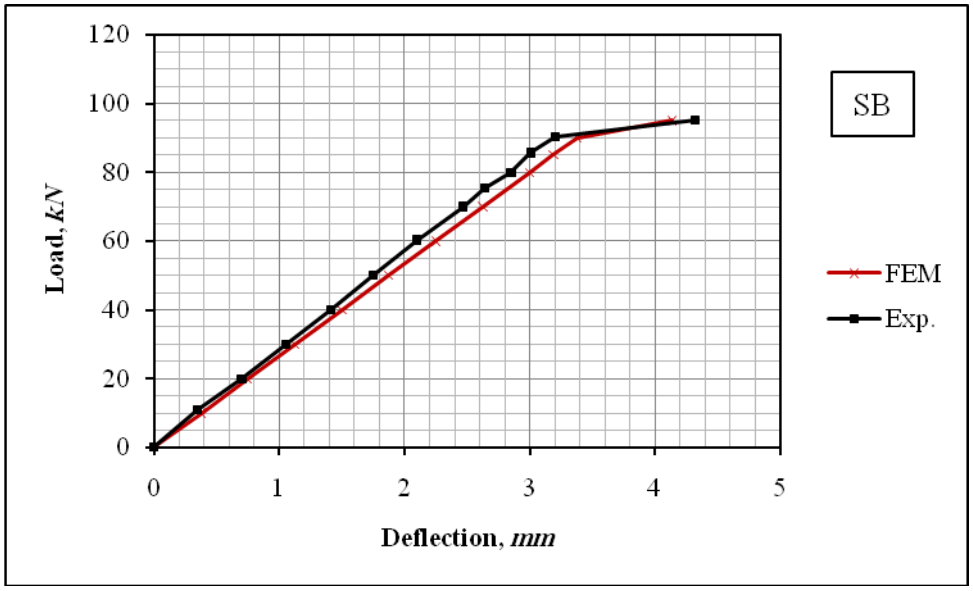

Fig.15: Load-deflection curves for tested PHC slab SB (At point A of max. deflections)

4.2. Crack Pattern and Modes of Failure

After the initiation of shear cracks, the stiffness of the tested PHC slabs was reduced and the load-deflection behavior ended when the failure occurs. In the actual slabs, the failure is abrupt and noisy, like a small explosion. In the actual and finite element models before failure, the failure zone is completely un-cracked. When the first crack appears, the failure takes places immediately. Figure 16 shows the evolution of crack patterns developing for each slab at the failure.

The failure modes of the finite element models show a good agreement with observations and data from the experimental full-scale slabs. In the actual slabs the failure mode appearing as web shear failure near the support for tested slab SA and flexural shear failure under the

vertical load for the tested slab SB. In the finite element models, the failure mode appears as shear failure under vertical load for both slabs.

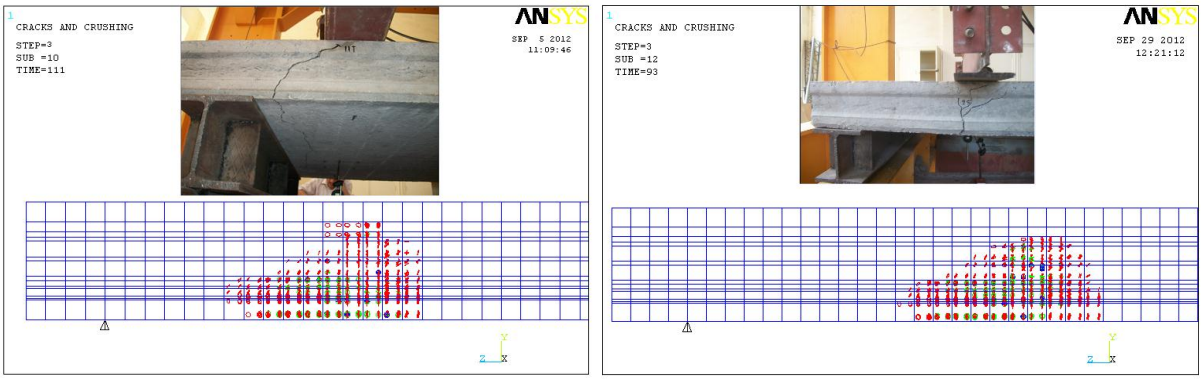

Fig.16: Side crack pattern and failure modes for tested PHC slab SA and SB

From the above verification, it can be conclude that the developed finite element model showed a good agreement between the experimental load deflection relationship, failure load, and cracks results. This indicates that the developed numerical models in the current study accurately predicted. Therefore, the developed finite element model for this research is given more confidence in the use of ANSYS program and suitable for use in further parametric studies.

5. Theoretical Analyses

This section presents the results of the parametric study conducted using the developed finite element model as presented above. The study investigates the effect of two key parameters that are expected to influence the shear capacity of PHC slabs. Those two parameters are the ratio of the load width imposed on slabs cross section and the shear span of the simply supported slabs.

The used model in this parametric study had the same geometric details, concrete and strand material properties of the model that is presented to simulate slab.

The studied variables are altered with a wide range to practically cover the effect of the parameter on the shear behavior of the PHC slabs. Outputs from model solutions are compared in terms of the load at first cracks. The following sections outline these results and the discussion for the investigated parameters.

5.1. Effect of Shear Span

There is a lack of research data in the literature about the critical shear span for the minimum diagonal shear resistance of PHC slabs. Bartlett and Macgregor [11] pointed out that the diagonal shear cracks are most critical when the shear span-to-depth ratio is around 2.5 (this conclusion was derived from the experimental work on regularly non-prestressed reinforced beams, which could have different behavior from PHC slabs). Cheng and Wang [6] presented data about the effect of shear span in 200 *mm* PHC slabs with circular voids. There was no data found regarding effect of shear span on other slabs with non-circular voids. Therefore, this study will investigate the effect of shear span on the shear capacity of slabs with non-circular voids and the developed FEM is used for this purpose. This investigation is performed by changing the location of the applied vertical line load on the model. The shear span is related to the average depth of slabs (h = 150 *mm*) by the shear span-to-depth ratio (a/h). Different a/h ratios, ranged from 2.0 to 6.0, are investigated. The load-deflection results

from this parametric study are presented for slabs plotted at the mid-point of the slab. The obtained load deflection graphs for the slab are shown in Fig.17.

a/h	Failure load *kN*
2	110
3	92
4	84
5	81
6	79

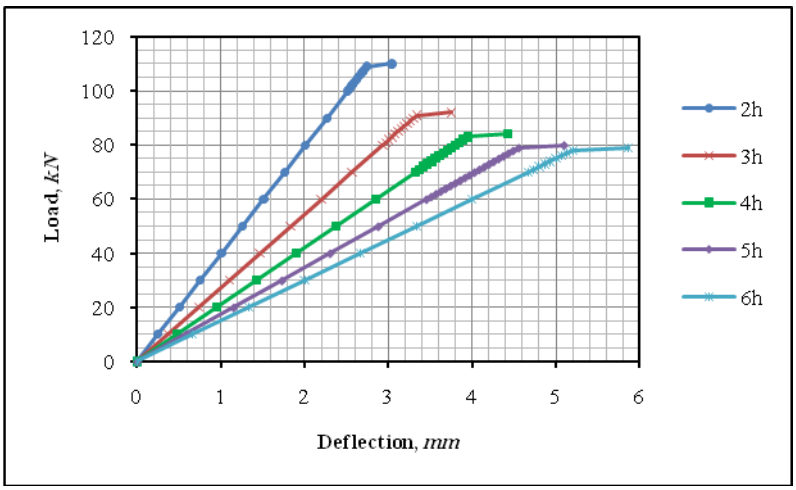

Fig.17: Load-deflection curves for different shear span of PHC slab

As expected, the deflection increased with increasing the shear span. Figure 18 presents ultimate failure loads versus the a/h ratio. According to the results of this conducted parametric study, it can be observed that the most critical shear capacity for the simulated 150 *mm* PHC slab with non-circular voids has decreased by increasing the shear span. From Figure 18, it can be observed that the shear capacity decreased significantly and clear with increasing the shear span, when value of shear span reached 4h and more, the shear capacity began decreasing slightly. The slab appeared to have higher shear capacity with a/h values smaller than 4. The increase in the shear capacity was 30% in case of a/h = 2 more than case of a/h = 4. On the other hand, the application of the load at a a/h > 4 would be less critical as flexural and shear or even flexural failure, where it governs the mode of failure. Moreover, the shear capacity was 3.7% lesser than in case of a/h = 5, which appeared to fail due to flexural and shear mode.

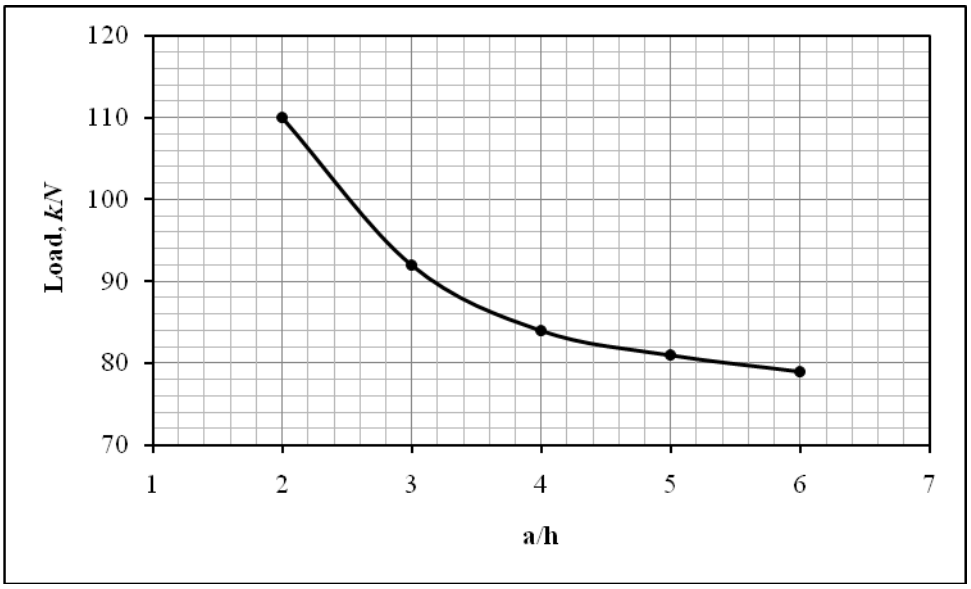

Fig.18: Ultimate failure loads versus the a/h ratio

5.2. Effect of Load Width

To study the effect of the load width on the shear capacity of the PHC slab, the level of load width was presented through nine cases for every shear span. The load width (b_L) ranged from 1200 to 416 mm, as shown in Table 3, while the shear span (a) is taken as 2, 3, 4 and 5h, respectively. The ultimate strength of full width of applied load is taken as the control case for each the other shear span to comparing the other results. These different levels of load width are simulated by changing the width of the applied load, which is symmetrically with the longitudinal axis of the tested slabs.

Table 3 summarizes the cracking and failure load obtained from the theoretical study. The results shown in the Table 3 indicated the significant effect of the applied load width, and show that capacity decreased with decreasing the load width. In addition, it can be observed from Figure 19, that the load-deflection curve is almost the same in all cases in elastic staged. On the other hand, it can be seen that whilst the applied load width is increasing, the brittle failure is occurred in all studied cases. This width of the load at which the failure to be brittle is changed by changing the shear span value. For example, increasing the shear span from 3 to 4h, the width ratio that the mode of failure transition to brittle failure are 43% and 50% respectively.

Table 3: Theoretical results for different load width versus the a/h ratio of slab

Load Width		**Slab** ($L = 3.5m$)							
b_L	(b_L/1200)	**P** at a = 2h		**P** at a = 3h		**P** at a = 4h		**P** at a = 5h	
	%	$\mathbf{P}_{Cracks}$	$\mathbf{P}_{Failure}$	$\mathbf{P}_{Cracks}$	$\mathbf{P}_{Failure}$	$\mathbf{P}_{Cracks}$	$\mathbf{P}_{Failure}$	$\mathbf{P}_{Cracks}$	$\mathbf{P}_{Failure}$
1200	100	108	110	90	92	82	84	78	81
1039	86.5833	108	110	90	92	82	84	78	80
950	79.1667	105	108	88	90	81	83	77	79
861	71.75	102	105	86	88	79	82	76	78
772	64.3333	99	102	84	86	78	80	75	78
683	56.9167	95	98	82	84	76	79	73	75~77
594	49.5	92	94	80	82	74	76~79	72	74~76
505	42.0833	88	92	77	79~81	72	74~79	70	72~76
416	34.6667	84	87	75	76~81	70	72~73	69	70~75

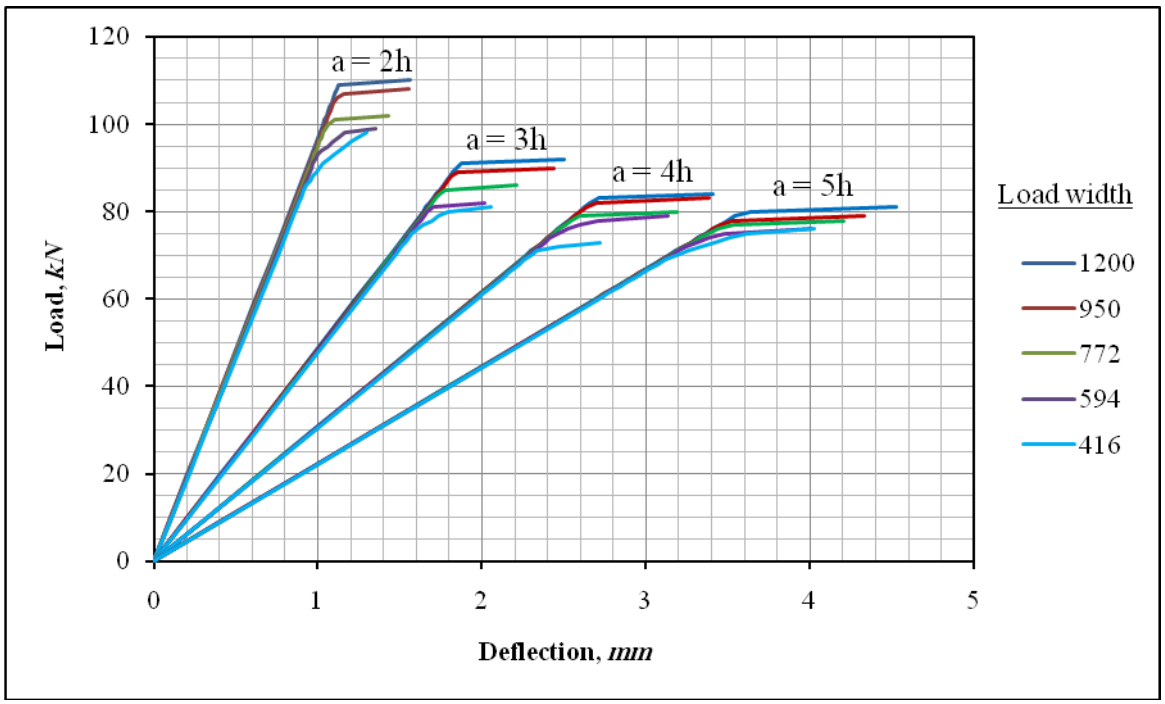

Fig.19: Load-deflection curves for different load width versus the a/h ratio of slab

6. Conclusions

Based on the obtained results and discussion, the following main conclusions are extracted:

- The numerical solution was adopted to evaluate the ultimate shear strength of prestressed hollow core slabs reinforced with eight prestressing strands, and compared with experimental full-scale test.
- The developed finite element model in this research can accurately simulate the shear behavior of prestressed concrete hollow core slab.
- The present finite element model can be used in future studies to develop design rules for prestressing hollow core slab members.
- The shear capacity of the slab decreased significantly and clear with increasing the shear span, this decreasing was 30% with increasing the shear span from 2h to 4h. After this value, the shear capacity began decreasing more slightly.
- Increasing of the load width is lead to increase the shear capacity of the slab then the failure go to brittle failure.

References

[1] MattiPajari, "Web shear failure in prestressed hollow core slabs", "Rakenteiden Mekanika (Journal of Structural Mechanics)", Vol. 42, No 4, 2009, pp. 207-217

[2] N. M. Hawkins and S. K. Ghosh; "Shear strength of hollow-core slabs", PCI Journal, January–February 2006, pp. 110–114.

[3] K. A. Truderung, "Shear capacity of dry-cast extruded precast prestressed hollow core slabs", PhD Thesis, University of Manitoba, Canada, 2011.

[4] L. Yang, "Design of prestressed hollow core slabs with reference to web shear failure", "ASCE Journal of Structural Engineering". 1994. Vol. 120, No. 9, pp. 2675–2696.

[5] A. J. Wolanski, "Flexural behavior of reinforced and prestressed concrete beams using finite element analysis". MSC Thesis, Milwaukee, Wisconsin, May, 2004

[6] S. Cheng and X. Wang; "Impact of interaction between adjacent webs on the shear strength of prestressed concrete hollow-core units", PCI Journal. 2010. Vol. 55, No. 3, pp. 46-63.
[7] ANSYS User's Manual, Version (11.0).
[8] A. M. Ibrahim and H. M. Mubarak; "Finite element modeling of continuous reinforced concrete beam with external pre-stressed", European Journal of Scientific Research ISSN 1450-216X. Vol.30, No.1, (2009), pp: 177-186.
[9] A. Deeb, M. Tarkhan and E. El-Tehewy; "Finite element modeling of pre-stressed hollow core slabs", International Conference on Civil and Architecture Engineering. Military Technical College. Egypt, Cairo 2012.
[10] ACI Committee 318, Building Code requirements for structural concrete (ACI 318-08) and Commentary (ACI 318R-08). "American Concrete Institute". Farmington Hills. Michigan. January 2008.
[11] J. G. Macgregor and F. M. Bartlett; "Reinforced Concrete Mechanics and Design", First Canadian Edition. Prentice Hall Canada Inc., Toronto. ON, Canada. 2000.